Force spectroscopy with a large dynamic range using small cantilevers and an array detector

Tilman E. Schäffer[a]

Department of Molecular Biology, Max-Planck-Institute for Biophysical Chemistry, 37077 Göttingen, Germany

The important characteristics of a detector for force spectroscopy measurements are sensitivity, linearity and dynamic range. The commonly used two-segment detector that measures the position of a light beam reflected from the force-sensing cantilever in an atomic force microscope becomes nonlinear when the beam shifts significantly onto one of the segments. For a detection setup optimized for high sensitivity, such as needed for the use with small cantilevers, it is shown both experimentally and theoretically that the dynamic range extends to an upper detection limit of only about 115 nm in cantilever deflection if $<10\%$ nonlinearity is required. A detector is presented that circumvents that limitation. This detector is based on a linear arrangement of multiple photodiode segments that are read out individually. With such an array detector, the irradiance distribution of the reflected beam is measured. The reflected beam not only shifts in position but also deforms when the cantilever deflects because the bent cantilever acts as a curved mirror. The mean of the distribution, however, is a linear function of cantilever deflection in both theory and experiment. An array detector is consequently well suited for force measurements for which both high sensitivity and a large dynamic range are required. © *2002 American Institute of Physics.*
[DOI: 10.1063/1.1450258]

I. INTRODUCTION

One of the unique properties of the atomic force microscope (AFM)[1] is its capability to measure picoNewton forces between a sharp tip and a sample surface. Forces are detected via the deflection of a flexible cantilever. Both high-sensitivity and a large dynamic range of the detection are important for force spectroscopy experiments, in which the force is recorded as a function of the tip–sample distance. Recently, a large number of single-molecule force spectroscopy experiments have been performed.[2–4] Small spring constants down to 10 mN/m are used for measurements of small forces. Forces were measured in the range of 9–20 pN for DNA base pairing,[5] in the range of 50–400 pN for ligand-receptor pairs,[3] in the range of 25–300 pN for intramolecular structural transitions of proteins[4] and up to 1–2 nN for covalent bonds.[6,7] Large spring constants of several tens of Newtons per meter are used for measurements of high forces: in nanoindentation measurements, for example, micromechanical sample properties are determined by indenting the sample with loading forces up to several tens of microNewtons.[8,9] A simultaneous high sensitivity and a large dynamic range are especially important when using cantilevers to measure surface stress such as in chemical or thermal sensors.[10–13]

One of the simplest and most sensitive techniques for the detection of cantilever deflections is based on optical beam deflection (''optical lever''), using a two-segment (split) photodetector.[14,15] One of the drawbacks of this detector, however, is its limited dynamic range. The latter is defined as

the measurement range between a lower and an upper detection limit over which cantilever deflections can be measured. The lower detection limit is defined as the smallest measurable deflection. The upper detection limit is defined as the cantilever deflection for which the signal deviates to a specified extend (e.g., 10%) from a linear response. A large dynamic range is necessary if the deflections vary greatly in magnitude.

There is a compromise, however, between a small lower detection limit and a large upper detection limit of the two-segment detector. It will be shown in this article that the parameter mediating this compromise is the focused spot diameter on the cantilever. A large focused spot diameter leads to a small lower detection limit (i.e., a high sensitivity) but also a small upper detection limit. A small focused spot diameter causes a large lower detection limit (i.e., a low sensitivity) but also a large upper detection limit. For regular-sized cantilevers, the upper detection limit can be increased by decreasing the focused spot diameter but at the sacrifice of detection sensitivity. Unfortunately, small, low-noise cantilevers do not allow significant variation in the focused spot diameter.[16–18]

It was shown earlier that the lower detection limit can be reduced under certain circumstances by using an array detector.[19] Here, the focus will be on the linearity and dynamic range aspects at large cantilever deflections.

II. EXPERIMENT

An incident collimated laser beam of the wavelength $\lambda = 686 \pm 5$ nm from a single-mode laser diode was focused to a spot on the cantilever (Fig. 1). The one-dimensional pro-

---

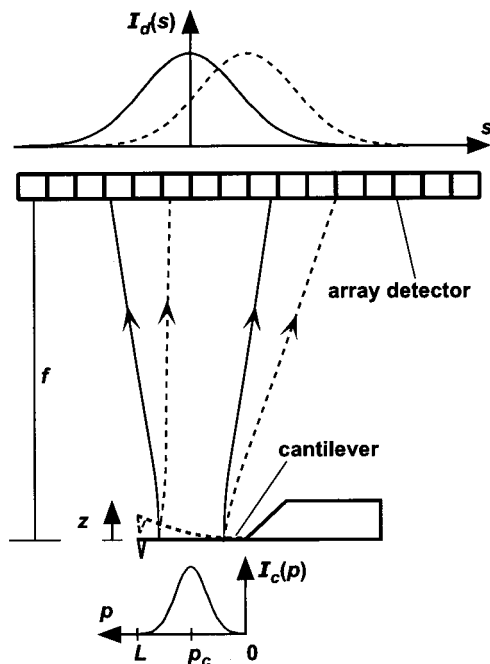[a]Electronic mail: tschaeff@gwdg.de

FIG. 1. Schematic of the detection setup with an array detector. An incident light beam was focused onto the cantilever, where it produced an irradiance distribution $I_c(p)$. The light reflected from the cantilever was projected onto the detector at distance f, where it produced a detector irradiance distribution $I_d(s)$ that was measured by the linear arrangement of the array detector of detector segments. When the cantilever deflected by z due to an applied force, the distribution shifted laterally.
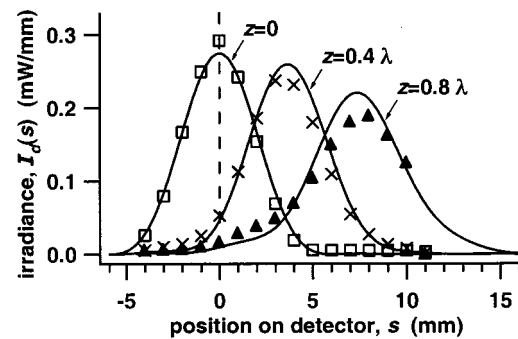

FIG. 2. Irradiance distribution of the reflected beam on the array detector at different cantilever deflections. At larger cantilever deflections ($z = 0.4\,\lambda$; $z = 0.8\,\lambda$), the reflected beam not only shifted laterally, but also increased in width and decreased in maximum irradiance. This is due to the fact that a bent cantilever acts as a curved mirror. Theoretical calculations (solid lines) match the experimental data.

jection of the irradiance distribution of the spot onto the p-axis, $I_c(p)$, had a Gaussian shape with a $1/e^2$ diameter of $w = 10 \pm 1\ \mu$m in the longitudinal direction of the cantilever and with a diameter of $5 \pm 0.5\ \mu$m along the width of the cantilever. An uncoated silicon nitride cantilever without an integrated probe tip was used, which was $L = 12 \pm 1\ \mu$m in length and $5 \pm 0.5\ \mu$m in width.[18] The focused spot was positioned between the clamped end of the cantilever ($p = 0$), referred to as base, and the free end of the cantilever ($p = L$), referred to as tip, such that the spot center was located at $p_c = 6 \pm 1\ \mu$m away from the cantilever base. The light beam reflected from the cantilever was projected onto the detector at the distance $f = 75 \pm 5$ mm from the cantilever, where it produced a spot with a light power of $P_{det} = 1.34 \pm 0.05$ mW and with an irradiance distribution $I_d(s)$. $I_d(s)$ denotes the one-dimensional projection of the irradiance distribution onto the s axis. The detector consisted of a linear array of 16 photodiode segments. In a previous study, the signals from the array detector segments were electronically added after selecting appropriate gain factors.[19] Here, the signals from the segments were read out individually using a multiplexer, allowing for the measurement of the detector irradiance distribution $I_d(s)$.

The cantilever was deflected by bringing its tip ($p = L$) into contact with a stiff sample surface (freshly cleaved mica in air) and vertically ramping up the sample with the help of a piezoelectric actuator positioned below the sample. This caused the spot on the detector to move. The resulting irradiance distribution $I_d(s)$ was recorded continuously as a function of cantilever deflection, z, and was plotted for three different cantilever deflections (Fig. 2). At zero cantilever deflection ($z = 0$), the irradiance distribution on the detector was symmetric and nearly Gaussian in shape (Fig. 2, rectangular markers). This was due to the Gaussian emission characteristics of the laser diode and to the fact that almost all of the incident light was reflected from the planar cantilever surface. When the cantilever was deflected vertically ($z = 0.4\,\lambda$), the spot translated laterally on the detector (Fig. 2, crossed markers). However, it not only changed in position but also in shape, i.e., with a decrease in height and an increase in width. At even larger cantilever deflections ($z = 0.8\,\lambda$), the spot further deformed (Fig. 2, triangular markers).

For the large cantilever deflections, it became apparent that the spot on the detector moved significantly away from where it was at zero deflection. A regular two-segment detector that simply detects the difference in power incident on the two segments (one segment at $s < 0$, the other one at $s > 0$) does not generate much variation in the difference signal at large cantilever deflections: It "loses sight" of the spot once the power of the spot has shifted predominantly onto one of the segments (e.g., compare $z = 0.4\,\lambda$ and $z = 0.8\,\lambda$ in Fig. 2).

The array detector, on the other hand, continues to track the spot up to large cantilever deflections, since it measures its complete irradiance distribution. The question is whether a suitable signal can be extracted from that distribution. In order for such a signal to be useful as a measure of cantilever deflection, it should be of high sensitivity and have a high linearity and a large dynamic range. In the following, first the theoretical lower and upper detection limit of a two-segment detector is derived. Then, a method is presented for the measurement of cantilever deflection by the array detector, utilizing the additional information obtained about the irradiance distribution.

III. THEORY

A. Irradiance distributions

The incident laser beam produces a focused spot on the cantilever with a one-dimensional Gaussian irradiance distribution in longitudinal direction of the cantilever (Fig. 1):

$$I_c(p) = \sqrt{\frac{8}{\pi}} \frac{P_0}{w} e^{-2[2(p-p_c)/w]^2}, \tag{1}$$

where P_0 is the total incident light power, w is the $1/e^2$ focused spot diameter, and p_c is the position of the center of the spot on the cantilever. According to Fraunhofer diffraction theory, the one-dimensional irradiance distribution on the detector is[20]

$$I_d(s,z) = \frac{k}{2\pi f} \left| \int_0^L dp \, E_c(p) e^{2ikzh(p)} e^{-iksp/f} \right|^2, \tag{2}$$

where $k = 2\pi/\lambda$ is the wave number of the incident light, λ is its wavelength, f is the distance from the cantilever to the detector, L is the length of the cantilever, $h(p)$ is its normalized shape, and z is the deflection at its tip ($p=L$). $E_c(p)$ is the scalar wave function of the light in the cantilever plane: $|E_c(p)|^2 = I_c(p)$. $E_c(p)$ is assumed to be real. It is required that the cantilever deflection be small compared to its length, $z \ll L$. This requirement allows the movement of the tip of the cantilever to be approximated as a vertical displacement only, without horizontal shift. At larger deflections, the horizontal position of the tip would move significantly toward the cantilever base, since the length of the cantilever is fixed. This requirement, $z \ll L$, is relaxed compared to the one used previously, in which $z \ll \lambda$ was required.[20] Equation (2) gives a good approximation of the detector irradiance distribution if the detector is placed in the far field of the reflected light beam, i.e., $f \gg \pi w^2/(2\lambda)$.

In force spectroscopy experiments, a force acts on the tip of the cantilever. Consider the normalized shape of a flexible, rectangular cantilever:[21]

$$h(p) = \frac{p^2(3L-p)}{2L^3} \tag{3}$$

$h(p)$ is normalized such that $h(0)=0$ and $h(L)=1$. It is due to this flexible nature of the cantilever that the detector irradiance distribution is distorted in size and in shape at larger cantilever deflections, because under such conditions the cantilever acts as a curved mirror. While some light is permitted to spill over the length of the cantilever (at its base and tip), it is assumed that no light spills over the width of the cantilever. The asymmetric spot needed to meet this requirement is often produced by the elliptical beam of the laser diode itself. This requirement permits the one-dimensional mathematical treatment of the system.

$I_d(s,z)$ is calculated numerically with parameters identical to the ones from the experiment ($w=10\,\mu$m, $p_c=6\,\mu$m, $f=75$ mm, $\lambda=686$ nm, $L=12\,\mu$m, and $P_{\text{det}}=1.34$ mW requiring $P_0=1.36$ mW). $I_d(s,z)$ is plotted at $z=0$, $z=0.4\,\lambda$, and $z=0.8\,\lambda$ (Fig.2, solid lines). At $z=0$, the theoretical irradiance distribution is nearly Gaussian in shape. At $z=0.4\,\lambda$, the center of the distribution is shifted to

the right-hand side but its height is decreased and its width increased. At $z=0.8\,\lambda$, the theoretical distribution further deforms and becomes asymmetric in shape: to the left-hand side of the peak of the distribution, a deflection point arises ($s\approx 1$ mm), due to diffraction effects. There is good agreement between the experimental and theoretical distributions. The theoretical distributions were generated by using only the measured experimental parameters. In particular, there are no free parameters in the theory and no curve fitting to the experimental curves was performed.

B. The two-segment detector

Expressions are now given for the lower and the upper detection limit of a conventional two-segment detector. The derivation presented here builds upon previous theoretical treatment,[20] where the effect of an adjustable aperture on the detection sensitivity was investigated.

The signal detected by a two-segment detector is the difference in light power incident on the two segments, $P_A - P_B$. To normalize the signal to a range of $[-1;1]$, $P_A - P_B$ is divided by the constant (time-averaged) total power incident on the detector, $P_{\text{det}} = P_A + P_B$. The difference signal, D, thus becomes

$$D(z) = \frac{P_A - P_B}{P_A + P_B} = \frac{1}{P_{\text{det}}} \int_{-\infty}^{+\infty} \text{sgn}(s) \, I_d(s,z) \, ds, \tag{4}$$

where $I_d(s,z)$ is the one-dimensional irradiance distribution on the detector [Eq. (2) and Fig. 1]. The detector was assumed to have 100% responsivity and to be large enough to detect all the light power reflected from the cantilever:

$$P_{\text{det}} = \int_0^L dp \, I_c(p). \tag{5}$$

When the cantilever deflection at its tip is small ($z \ll \lambda/(2\pi)$), the difference signal is linear in z,

$$D(z) = \frac{z}{z_{\text{max}}}, \tag{6}$$

where[20]

$$z_{\text{max}} = \lambda \left(\frac{4}{P_{\text{det}}} \int_0^L dp \int_0^L dp' E_c(p) \right.$$
$$\left. \times E_c(p') \frac{h(p)-h(p')}{p-p'} \right)^{-1}. \tag{7}$$

When the cantilever deflection becomes larger ($z > \lambda/(2\pi)$), $D(z)$ becomes nonlinear and Eq. (6) is no longer valid. This is because Eq. (6) requires the power shifted from one to the other segment to increase linearly with cantilever deflection. But less and less power shifts at increasing deflection due to finite spot size and power. For large deflections, when the spot on the detector is shifted by a large distance compared to its width, almost all of the power is incident onto one segment ($P_A \approx P_{\text{det}}$, $P_B \approx 0$), and the difference signal becomes saturated at $D(z) \approx 1$. Therefore, the two-segment detector has a finite upper detection limit. It can be shown that z_{max} corresponds to the upper detection limit if a nonlinearity of $<21.3\%$ is required. For the experimental
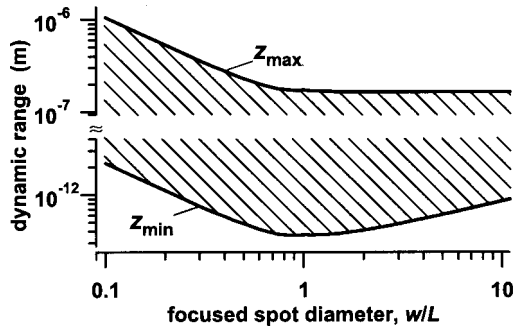
FIG. 3. Theoretical dynamic range of a two-segment detector as a function of the focused spot diameter. The dynamic range is the range between the lower and the upper detection limit (highlighted area). This points out the compromise between a small lower and a large upper detection limit (defined here for 21.2% nonlinearity): If the upper detection limit is increased by decreasing the focused spot diameter, the lower detection limit increases as well (for $w/L < 1$). Therefore, a large upper detection limit goes at the expense of low detection sensitivity.

parameters used, $z_{max} \approx 0.266 \, \lambda \approx 182$ nm [Eq. (7)]. Such a maximum detectable deflection is too small for many force spectroscopic applications.

The minimum detectable cantilever deflection, i.e., the lower detection limit, z_{min}, is obtained at a signal-to-noise ratio (SNR) of one: $D(z_{min})/N_r = 1$, where N_r is the fundamentally limiting photonic shot noise in the difference signal (root-mean-square power fluctuations as a fraction of the total power at the detector):

$$N_r = \sqrt{\frac{2hc\Delta f}{\lambda P_{det}}} = \sqrt{\frac{1}{n}}. \tag{8}$$

h is Planck's constant, c is the speed of light, and the dimensionless parameter n is the mean number of photons that are counted within the measurement bandwidth, Δf. Equation (8) reflects the fact that shot noise arises from photon counting and is described by Poisson statistics, where the variance of the number of counted photons equals the mean number of counted photons (note that the square of N_r is the shot-noise contribution to the relative intensity noise). The relative width of the dynamic range is calculated using Eq. (6):

$$\frac{z_{max}}{z_{min}} = \frac{1}{N_r} = \sqrt{n}. \tag{9}$$

It is therefore determined only by n, the number of photons counted within the measurement bandwidth, and is independent of the particular shape of the detector irradiance distribution.

For high-sensitivity detection, a large SNR is required and thus the lower detection limit, z_{min}, needs to be minimized. The focused spot diameter, w, has a strong effect on the lower detection limit. There is a compromise, however, between the lower and upper detection limit. To demonstrate this compromise, z_{min} and z_{max} are plotted versus. the normalized focused spot diameter, w/L (Fig. 3). The parameters used for this plot are $\Delta f = 10$ kHz and $P_0 = 1.36$ mW, again matching the experimental parameters. To make use of the

high-slope area at the tip of the deflected cantilever, the position of the focused spot on the cantilever was adjusted depending on the diameter of the spot:

$$p_c = \begin{cases} L - w/2; & w \leq L \\ L/2; & w > L \end{cases} \tag{10}$$

This somewhat arbitrary condition fixes one of the $1/e^2$ irradiance points to the tip of the cantilever, ensuring that a large fraction of the incident beam is incident close to the tip where deflections are largest and therefore approximately opimizing the detection sensitivity for the given spot diameter. It can be seen (Fig. 3) that for focused spot diameters smaller than the cantilever length ($w/L < 1$), z_{min} decreases for increasing spot diameters, reaching a minimum of $\approx 3.6 \times 10^{-13}$ m at $w/L \approx 0.9$. At this point, the detection sensitivity is highest. For spot diameters larger than the cantilever length ($w/L > 1$), z_{min} increases again, reflecting a reduced detection sensitivity due to light lost over the edges at the tip and the base of the cantilever. This confirms the finding that the detection sensitivity is optimized when the focused spot approximately fills the cantilever, justifying the choice of the focused spot diameter in the experiment.[22,23]

For focused spot diameters below the cantilever length ($w/L < 1$) it can be seen that z_{max} decreases with the same rate as z_{min} (Fig. 3). This is a manifestation of the compromise between a low-noise and a large-upper-limit detection [Eq. (9)]. For the parameters used in the experimental setup, $z_{max}/z_{min} \approx 4.8 \times 10^5$. The dynamic range therefore covers between 5 and 6 orders of magnitude of measurable cantilever deflection (highlighted area in Fig. 3, $w/L < 1$). For $w/L > 1$, light is lost over the edges of the cantilever and fewer photons will reach the detector, decreasing the dynamic range. It will be shown next that an array detector increases the upper detection limit without sacrificing detection sensitivity by simply increasing the number of detector segments.

Note that $p_c = 6 \, \mu$m was used in the experimental setup, which is slightly smaller than the 7 μm that would have been a better choice according to Eq. (10). Note also that there is a slight discontinuity in the slope of z_{min} and z_{max} at $w/L = 1$ (Fig. 3) due to the respective discontinuity of the slope of p_c [Eq. (10)].

C. The array detector

The mean (first moment), $\bar{s}(z)$, of the detector irradiance distribution, $I_d(s,z)$, is defined as

$$\bar{s}(z) = \frac{1}{P_{det}} \int_{-\infty}^{+\infty} s \, I_d(s,z) \, ds, \tag{11}$$

where a detector large enough to detect all light power reflected from the cantilever is assumed again. Mathematically, the only change to the difference signal of the two-segment detector, Eq. (4), is the replacement of "sgn(s)" by "s." This functional form yields an optimum measure of cantilever deflection for an approximately Gaussian detector irradiance profile.[19] Equation (11) can be expanded to

$$\bar{s}(z) = \frac{k}{2\pi f P_{det}} \int_0^L dp \int_0^L dp' \, E_c(p) E_c(p')$$

$$\times e^{2ikz[h(p)-h(p')]} \int_{-\infty}^{\infty} ds \, s \, e^{-iks(p-p')/f}. \quad (12)$$

Using the Dirac Delta function defined as $\delta(x) = 1/(2\pi)\int_{-\infty}^{\infty} e^{-isx} ds$ one obtains by partial integration with respect to p':

$$\bar{s}(z) = \frac{f}{ikP_{det}} \int_0^L dp \, E_c(p) e^{2ikzh(p)}$$

$$\times \left\{ [E_c(p') e^{-2ikzh(p')} \, \delta(p'-p)]_{p'=0}^L \right.$$

$$\left. - \int_0^L dp' \, \delta(p'-p) \frac{d}{dp'} [E_c(p') e^{-2ikzh(p')}] \right\}$$

$$= \frac{f}{ikP_{det}} \left\{ \frac{1}{2} [E_c^2(p)]_{p=0}^L \right.$$

$$\left. - \int_0^L dp \, E_c(p) e^{2ikzh(p)} \frac{d}{dp} [E_c(p) \, e^{-2ikzh(p)}] \right\}$$

$$= \frac{f}{ikP_{det}} \left\{ \frac{1}{2} [E_c^2(p)]_{p=0}^L - \int_0^L dp \, E_c(p) \, E_c'(p) \right.$$

$$\left. + 2ikz \int_0^L dp \, E_c^2(p) \, h'(p) \right\} \quad (13)$$

The factor 1/2 in the first term in the curly brackets arises because the integration over p covers only half of the (symmetric) Delta singularity at both $p=0$ and $p=L$. The first and second term in the last line cancel and the mean of the detector irradiance distribution simplifies to

$$\bar{s}(z) = \varepsilon \frac{2f}{L} z, \quad (14)$$

where the dimensionless parameter ε is

$$\varepsilon = \frac{L}{P_{det}} \int_0^L I_c(p) h'(p) dp. \quad (15)$$

Equation (14) relates the mean of the detector irradiance distribution, $\bar{s}(z)$, to the cantilever deflection, z. It can be seen that $\bar{s}(z)$ is linear in z. This is a result that is not obvious *a priori*, since the spot on the detector deforms at large deflections. Apparently, this does not affect the linearity of $\bar{s}(z)$. The parameter ε represents the deviation from a hypothetical setup with a planar cantilever $(h(p)=p/L)$ that extends beyond the base and the tip, such that all incident light is reflected $(\varepsilon=1)$. Comparing Eq. (14) with Eq. (6) indicates a similar linear relationship for both the array detector and the two-segment detector, but the array detector does not require small cantilever deflections, $z \ll \lambda/(2\pi)$. It is therefore capable of measuring larger cantilever deflections than the two-segment detector.

For the experimental parameters, $\varepsilon \approx 1.07$ and $\bar{s}(z) \approx (1.33 \times 10^4) \, z$. When the cantilever deflects by 1 nm, for example, the mean of the detector irradiance distribution

translates by ≈ 13.3 μm. Alternatively, one can also write $\bar{s}(z) \approx (9.15 \text{ mm}) \, z/\lambda$, i.e., the mean of the distribution moves by $\bar{s}(\lambda) \approx 9.15$ mm when the cantilever deflects by one wavelength, $z=\lambda$. Since this translation is similar in size to the width of the spot on the detector (7.4 mm, estimated at $z=0$ between the $1/e^2$ irradiance points), the translation of the spot on the detector is on the order of its width when the cantilever deflects by one wavelength. Even though this relation was derived for these particular experimental conditions, it also holds true for other choices of f, λ, L and w, as long as the focused spot diameter approximately fills the cantilever $(w/L \approx 1)$. When the focused spot on the cantilever becomes smaller, the width of the detector irradiance distribution becomes larger and the spot translates by a smaller fraction of its width for the same cantilever deflection, decreasing the detection sensitivity. According to Eq. (14), $\bar{s}(z)$ could be made arbitrarily large for a given z by increasing f, for example. But obviously this will not increase the precision in determining $\bar{s}$, since the spot width would also increase proportionally to f. The detection sensitivity would therefore remain the same.

IV. RESULTS AND DISCUSSION

The array detector is considered in comparison to the two-segment detector with respect to linearity and dynamic range. First, it is discussed how well the two-segment detector can measure large cantilever deflections. One can relate the measured cantilever deflection, z_m^{2SD}, to the actual, physical deflection, z, by rewriting Eq. (6) as

$$z_m^{2SD}(z) = z_{max} D(z). \quad (16)$$

$D(z)$ is the difference signal produced by the two-segment detector and z_{max} is the scaling factor for obtaining the quantitative measurement of the deflection, z_m^{2SD}, in units of meter. Equation (16) reflects the principle by which all deflection measurements using the conventional two-segment detector are being performed. It is possible to directly calculate z_{max} by using Eq. (7) (yielding a theoretical value of ≈ 182 nm), but instead, $z_{max}=160$ nm is determined experimentally by the usual calibration procedure in which the slope of he force curve ("force spectrum") in the linear range (here: 0 nm $\leq z \leq 50$ nm) is measured. This way, measurement inaccuracies of the experimental parameters (including z-piezo calibration) are neutralized, facilitating a comparison between the linearities of the two-segment detector and the array detector. $z_m^{2SD}(z)$ is plotted as a function of z (Fig. 4, diamond-shaped markers) with $D(z)$ determined from the measured detector irradiance profile. It can be seen that the measured cantilever deflection was linear only at small actual cantilever deflections ($z < 100$ nm). At larger actual deflections, the measured deflections became asymptotically limited at $z_{max} \approx 160$ nm, reflecting the fact that the difference signal, $D(z)$, approached unity. One can define a nonlinearity coefficient, χ, as

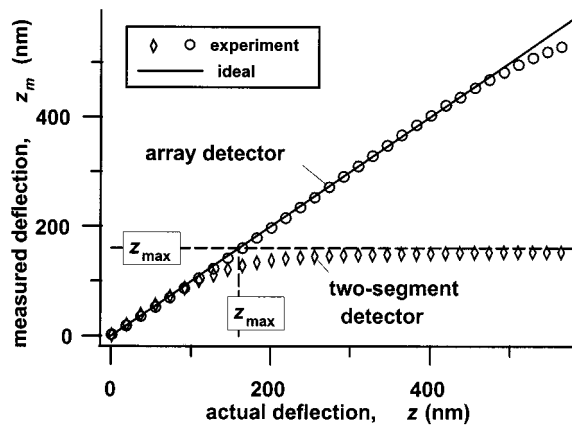$$\chi = 1 - \frac{z_m}{z}, \quad (17)$$

FIG. 4. A force curve recorded by the two-segment detector and by the array detector. In the case of the two-segment detector (diamond-shaped markers), the measured cantilever deflection became 10% nonlinear at an actual cantilever deflection of 115 nm. For the array detector, the measured deflection stayed within 10% nonlinearity up to 580 nm (circular markers), even though the detector irradiance distribution became quite distorted (Fig. 2, triangular markers). But this nonlinear deviation above 580 nm is only due to the fact that the spot on the detector moved beyond the active detector area. Adding more segments would keep a linear dependency for even larger deflections, as the ideal curve indicates (solid line).

with z_m/z being the ratio of measured to actual cantilever deflections. χ is zero for a perfectly linear response. From Fig. 4 (diamond-shaped markers), it follows that the signal became 10% nonlinear at an actual cantilever deflection of ≈ 115 nm. When the cantilever was further deflected, the signal became 21.3% nonlinear at an actual cantilever deflection of ≈ 161 nm ($\approx z_{max}$) and finally became saturated at even larger deflections. This saturation was not electronic in nature, but was rather due to the spot being shifted all the way onto one of the two segments. Even though it is possible in principle to generate a nonlinear correction curve via a calibration force curve, a linear dependency is preferred because it is easier to work with and because a correction would increase the noise of the measurement. Therefore, saturation is inherent to the two-segment detector. These results imply that when using a setup optimized for high sensitivity and a cantilever with a flexural spring constant of 10 mN/m, the upper detection limit is reached at a force of only 1–2 nN. This force is smaller than those of interest in many applications.

The array detector can be discussed in a similar manner, i.e., with respect to how well it can measure large cantilever deflections. For that purpose, relate the measured cantilever deflection, z_m^{AD}, to the actual, physical deflection, z, by rewriting Eq. (14) as

$$z_m^{AD}(z) = \frac{L}{2f\epsilon} \bar{s}(z). \tag{18}$$

$\bar{s}(z)$ is the signal produced by the array detector and $L/(2f\epsilon)$ is the scaling factor for obtaining the quantitative measurement of the deflection, z_m^{AD}, in units of meter. Just as in the case of the two-segment detector, this scaling factor could be directly calculated using Eq. (15) (yielding a theoretical value of $\approx 7.50 \times 10^{-5}$), but instead, $L/(2f\epsilon) \approx 8.15 \times 10^{-5}$ is determined experimentally by a calibration proce-

dure, in which the slope of the force curve in the linear range (here: 0 nm $\leq z \leq$ 400 nm) is measured. $z_m^{AD}(z)$ is plotted as a function of z (Fig. 4, circular markers), with $\bar{s}(z)$ determined from the measured detector irradiance profile. It can be seen that the measured cantilever deflection was linear up to much larger deflections than it was in the case of the two-segment detector. Only at actual deflections over 500 nm, the measured deflection, z_m^{AD}, started to deviate from a linear curve with unit slope (Fig. 4, solid line). This, however, is simply due to the fact that the spot moved beyond the active detector area (see also Fig. 2). A linear behavior would be maintained for much larger deflections if the number of segments were increased to cover a larger area. The missing probe tip and the resulting variability in the sample contact could account for some deviations of the experimental values from the ideal curve at deflections below 500 nm (Fig. 4).

The fact that the scaling factor that relates measured cantilever deflection to the signal from the detector could be calculated using Eq. (16) for the two-segment detector or Eq. (18) for the array detector, respectively, suggests that the experimental calibration procedure, in which a physical force curve is acquired on a hard surface, might be avoided entirely. It may simply be necessary to calculate the respective scaling factor using the experimental parameters (L, w, p_c, λ, f) measured up to the required accuracy. This would have the advantage that the force-sensing tip would not have to be brought into contact with any surface before the actual measurement, therefore simplifying the experiment and avoiding possible tip contamination. The spring constant of the cantilever, for example, could then directly be determined from a thermal noise spectrum,[24,25] without the need for the preceding calibration measurement. One practical problem with this approach is that the focused spot needs to be accurately placed on the cantilever. The error in slope introduced by this placement uncertainty is estimated to be about 5%. Furthermore, in AFM setups for use with liquids, the quality and size of the spot on the detector is affected by optical media and interfaces in the beam path (e.g., the liquid cell). The array detector, however, could be used to perform an immediate "spot quality" assessment similar to the method of D'Costa and Hoh,[26] with the advantage that the detector would not have to be moved manually.

In the theory, a functional shape of the cantilever was chosen that reflects a quasistatic force acting on the tip. This choice is validated by the good agreement between experimental and theoretical values in Fig. 2. During dynamic microscope operation, however, the detailed motion of the cantilever is more complex. For example, dynamic instabilities close to the sample surface can occur in force curves, distorting the cantilever shape.[27] An array detector might be useful for deducing the functional shape of the cantilever during such dynamic processes directly from the detector irradiance profile.

It was mentioned that adding more segments to the array detector increases its upper detection limit. For the number of segments used here, the measured deflection became 10% nonlinear (with respect to its linear fit) at an actual deflection of ≈ 580 nm. Therefore, if $<10\%$ nonlinearity is required within the dynamic range, the upper detection limit was mea-

sured to be larger by a ratio of $580/115 \approx 5.0$ for the array detector than for the two-segment detector. One could easily increase this ratio by simply adding more segments to the array detector. However, the ratio is theoretically limited by the requirement $z \ll L$ [Eq. (2)]. Relating this requirement to that for the two- segment detector, $z \ll \lambda/(2\pi)$ [Eq. (6)], one estimates a maximum ratio of $2\pi L/\lambda \approx 110$. This would raise the upper detection limit (at $<10\%$ nonlinearity) of the array detector to approximately 13 μm. Another limitation that becomes important for small cantilevers is given by the geometric arrangement of the cantilever with respect to the surface: The support chip crashes into the surface at $z_{crash} = L\sin(\alpha) + l_t\cos(\alpha)$, where α is the tilt of the cantilever with respect to the surface and l_t is the length of the tip. For a small cantilever (e.g., $L=12$ μm), the maximum deflection is $z_{crash} \approx 6.0$ μm, compared to $z_{crash} \approx 21$ μm for a large cantilever ($L=100$ μm) (using a typical tilt of $\alpha=10°$ and a tip length of 4 μm).

A continuous detector irradiance distribution was assumed in the theoretical calculation of its mean. In the experiment, there are slightly different conditions, because the distribution was integrated over the finite size of each segment. If the width of the distribution were small compared to the segment size, the measured mean would not be linear in cantilever deflection but would exhibit a step-like behavior. This effect occurs because such a case resembles the behavior of a two-segment detector, with contributions to the mean only when the narrow distribution crosses a segment boundary. In the case of a Gaussian distribution profile with a $1/e^2$ width of at least twice the segment size, it is estimated from a simple calculation (data not shown) that the deviation of the mean in both slope and absolute value is below 1% of the true values. Since the $1/e^2$ width of the distribution at $z=0$ in Fig. 2 is approximately 7.4 times the segment size, such an effect was entirely neglected here.

It was shown for a special case that the lower detection limit, z_{min}, was lower by a ratio of ≈ 5 for the array detector compared to the two-segment detector, making the array detector suitable for high-sensitivity detection.[19] For a Gaussian focused irradiance profile like the one used here, this ratio decreased to approximately 1.25. The lower detection limit, z_{min}, was calculated as $\approx 3.6 \times 10^{-13}$ m $=0.0036$ Å. Experimentally, a deflection this small could not be detected, because other noise sources (such as laser noise) contribute significantly. Therefore, the relative width of the dynamic range, Eq. (9), was mostly determined by z_{max}. It is not possible, however, to change an experimental parameter such as the focused spot diameter in order to raise the theoretical lower detection limit to the level of the experimental lower detection limit, with the intention of increasing the experimental dynamic range at the same detection sensitivity. Such a procedure does not work because the experimental lower detection limit also increases by this procedure. In general, the highest experimental sensitivity is achieved for the highest theoretical sensitivity. Also, in the case of small cantilevers, one cannot easily decrease the focused spot diameter to gain dynamic range because of optical limitations.

In the theory for the two-segment detector, it was found that the relative width of the dynamic range was 4.8×10^5. In practice, however, an analog-to-digital converter that samples the difference signal with a bit depth of typically 16 can provide a relative width of at most $2^{16} \approx 6.6 \times 10^4$. If 0.05 Å were the lowest deflection that could be sampled, then the practical dynamic range would be at most 330 nm. The array detector, on the other hand, does not have such a sampling limitation, since $\bar{s}(z)$ is calculated from the digitized signals from many segments.

V. CONCLUSION

An array detector combines a high sensitivity and a large dynamic range. Its lower detection limit is comparable to or smaller than that of a two-segment detector, and its upper detection limit is only restricted by the size of the detector and by geometrical constraints of the cantilever. Therefore, an array detector overcomes the relatively small upper detection limit of the two-segment detector without sacrificing sensitivity. In the particular case of a small cantilever with a focused spot diameter nearly optimized for high-sensitivity detection, the experimental upper detection limit (at 10% nonlinearity) was increased from 115 nm for a two-segment detector to 580 nm for an array detector. Theoretically, the upper detection limit could be increased up to 13 μm by increasing the number of array detector segments. The mean of the detector irradiance distribution is a linear function of cantilever deflection, even though the shape of the distribution becomes distorted at larger deflections. In addition to having a large dynamic range, no mechanical adjustments such as centering the beam on the detector are required for an array detector.

[1] G. Binnig, C. F. Quate, and C. Gerber, Phys. Rev. Lett. **56**, 930 (1986).
[2] H. Clausen-Schaumann, M. Seitz, R. Krautbauer, and H. E. Gaub, Curr. Opin. Chem. Biol. **4**, 524 (2000).
[3] J. Zlatanova, S. M. Lindsay, and S. H. Leuba, Prog. Biophys. Mol. Biol. **74**, 37 (2000).
[4] A. Janshoff, M. Neitzert, Y. Oberdörfer, and H. Fuchs, Angew. Chem. Int. Ed. Engl. **39**, 3213 (2000).
[5] M. Rief, H. Clausen-Schaumann, and H. E. Gaub, Nat. Struct. Biol. **6**, 346 (1999).
[6] M. Grandbois, M. Beyer, M. Rief, H. Clausen-Schaumann, and H. E. Gaub, Science **283**, 1727 (1999).
[7] M. A. Lantz, H. J. Hug, R. Hoffmann, P. J. A. van Schendel, P. Kappenberger, S. Martin, A. Baratoff, and H. J. Güntherodt, Science **291**, 2580 (2001).
[8] N. A. Burnham and R. J. Colton, J. Vac. Sci. Technol. A **7**, 2906 (1989).
[9] B. Bhushan and V. N. Koinkar, Appl. Phys. Lett. **64**, 1653 (1994).
[10] T. Thundat, R. J. Warmack, G. Y. Chen, and D. P. Allison, Appl. Phys. Lett. **64**, 2894 (1994).

[11] H. J. Butt, J. Colloid Interface Sci. **180**, 251 (1996).

[12] R. Berger, E. Delamarche, H. P. Lang, C. Gerber, J. K. Gimzewski, E. Meyer, and H. J. Güntherodt, Science **276**, 2021 (1997).

[13] T. Miyatani and M. Fujihira, J. Appl. Phys. **81**, 7099 (1997).

[14] G. Meyer and N. M. Amer, Appl. Phys. Lett. **53**, 1045 (1988).

[15] S. Alexander, L. Hellemans, O. Marti, J. Schneir, V. Elings, P. K. Hansma, M. Longmire, and J. Gurley, J. Appl. Phys. **65**, 164 (1989).

[16] D. A. Walters, J. P. Cleveland, N. H. Thomson, P. K. Hansma, M. A. Wendman, G. Gurley, and V. Elings, Rev. Sci. Instrum. **67**, 3583 (1996).

[17] T. E. Schäffer, J. P. Cleveland, F. Ohnesorge, D. A. Walters, and P. K. Hansma, J. Appl. Phys. **80**, 3622 (1996).

[18] M. B. Viani, T. E. Schäffer, A. Chand, M. Rief, H. E. Gaub, and P. K. Hansma, J. Appl. Phys. **86**, 2258 (1999).

[19] T. E. Schäffer, M. Richter, and M. B. Viani, Appl. Phys. Lett. **76**, 3644 (2000).

[20] T. E. Schäffer and P. K. Hansma, J. Appl. Phys. **84**, 4661 (1998).

[21] D. Sarid, *Scanning Force Microscopy: With Applications to Electric, Magnetic, and Atomic Forces*, 2nd ed. (Oxford University Press, New York, 1994).

[22] C. A. J. Putman, B. G. De Grooth, N. F. Van Hulst, and J. Greve, J. Appl. Phys. **72**, 6 (1992).

[23] M. G. L. Gustafsson and J. Clarke, J. Appl. Phys. **76**, 172 (1994).

[24] J. L. Hutter and J. Bechhoefer, Rev. Sci. Instrum. **64**, 1868 (1993).

[25] H. J. Butt and M. Jaschke, Nanotechnology **6**, 1 (1995).

[26] N. P. D'Costa and J. H. Hoh, Rev. Sci. Instrum. **66**, 5096 (1995).

[27] B. A. Todd, S. J. Eppell, and F. R. Zypman, Appl. Phys. Lett. **79**, 1888 (2001).